

Developing an Experimental Week 2–4 Severe Weather Outlook for the United States

Hui Wang¹, Alima Diawara^{1,2}, Arun Kumar¹, David DeWitt¹

¹Climate Prediction Center, NOAA/NWS/NCEP, College Park, MD

²Innovim, LLC, Greenbelt, MD

1. Introduction

Developing week 2 to 4 severe weather outlooks is one of the CPC projects under the Office of Science and Technology Policy initiative. The goals of this project are (1) to expand development and perform evaluation of week-2 severe weather model guidance in the first year, and (2) to explore the potential and develop experimental forecast tools for week 3 and 4 severe weather in the second year. The results presented at the workshop focus on week 2 forecast.

Based on different timescales, forecasts can be categorized into three types. One is short-term prediction for several days, mainly determined by initial conditions. Another is seasonal outlook from one month to several seasons. At this timescale, slow evolving components, such as SST, ENSO and AMO, are the sources of predictability. In-between is the extended-range prediction from week 2 to week 4. At this time range, the forecast skill is relatively low mainly due to a lack of source of predictability.

A recent study by Carbin *et al.* (2016) uses the Supercell Composite Parameter (SCP) derived from the CFSv2 45-day forecast to provide extended-range severe weather environment guidance. When SCP is greater than **one**, it is expected that severe weather will likely occur. Here we take one more step to forecast severe weather based on empirical relationship between model predicted SCP and actual severe weather in historical records.

2. Data and methods

The data used in this study consist of both observational data and model forecast. For observations, the Climate Forecast System Reanalysis (CFSR) and local storm report (LSR) are employed. The LSR includes hail, tornado, and damaging wind, as well as their location, time and intensity. The sum of the LSRs for hail, tornado and damaging wind are referred to as LSR3 hereafter. They are re-gridded to a $0.5^\circ \times 0.5^\circ$ grid. We use the NCEP GEFS 16-day hindcasts for week 2. Hindcast period is from 1996 to 2012. The hindcasts were made every 4 days with 5 members and a $0.5^\circ \times 0.5^\circ$ resolution. The analysis presented was performed with the 5-member ensemble mean.

Following Carbin *et al.* (2016),

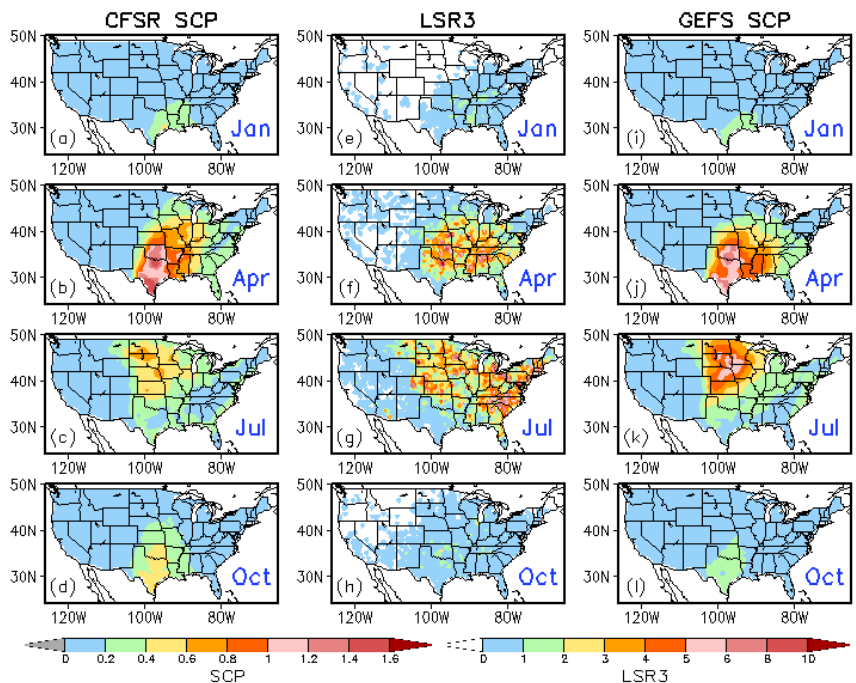


Fig. 1 Climatological monthly mean daily SCP for January, April, July and October derived from (a–d) CFSR and (i–l) GEFS day-1 forecast and (e–h) observed climatological monthly LSR3 in the period of 1996–2012.

the SCP is defined as

$$\text{SCP} = (\text{CAPE}/1000 \text{ J kg}^{-1}) \times (\text{SRH}/50 \text{ m}^{-2} \text{ s}^{-2}) \times (\text{BWD}/20 \text{ m s}^{-1}),$$

where CAPE is convective available potential energy, SRH storm-relative helicity, and BWD bulk wind difference. The three constants are used to normalize SCP so that when SCP is greater than 1, there is a chance for severe weather to occur.

The forecast model developed in this study is a hybrid dynamical-statistical model (e.g., Wang *et al.* 2009). It uses the dynamical model (GEFS) predicted SCP as a predictor, and then forecast severe weather (LSR3) based on the statistical relationship between model SCP and actual LSR3 in historical records. The forecast skill is cross-validated over the GEFS hindcast period (1996–2012).

3. Results

The observed seasonality of SCP is examined first. Figure 1a–d shows the climatological monthly mean daily SCP over the U.S. for January, April, July, and October, respectively, derived from CFSR. The seasonal variation of SCP is characterized by relatively large values of SCP appearing in the Gulf States during winter months. Then SCP intensifies and peaks in spring. The region of the maximums moves northward from the Southern Plain in spring to the Northern Plain in summer. From summer to the following winter, the SCP value decreases and the center of the maximums moves back to the south. The SCP displays strong seasonality over the central U.S. Over the same region, the LSR3 also shows similar seasonality with strong severe weather activity in spring and summer (Fig. 1e–h). During these two seasons, however, there are also strong activities in the eastern U.S. where SCP value is small. Therefore, in terms of seasonal cycle, there is a good correspondence between SCP and LSR3 in the central U.S.

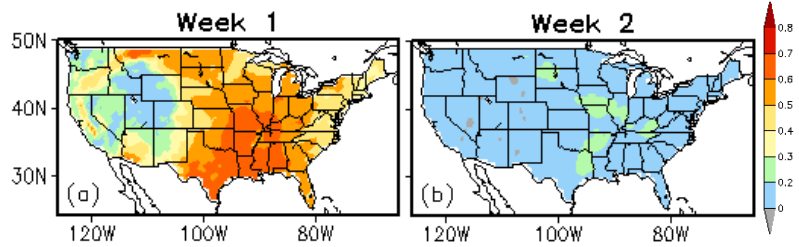


Fig. 2 Anomaly correlation between SCPs from CFSR and GEFS hindcasts for (a) week 1 and (b) week 2 over the 1996–2012 period.

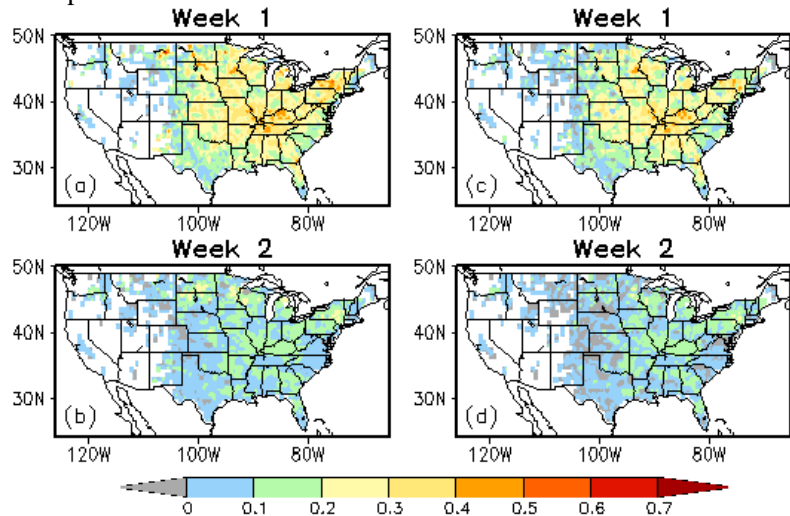


Fig. 3 Correlations between observed LSR3 and SCP from the GEFS hindcasts for (a) week 1 and (b) week 2 and anomaly correlations between observed LSR3 and predicted LSR3 from the dynamical-statistical model for (c) week 1 and (d) week 2 based on cross-validations over the 1996–2012 GEFS hindcast period.

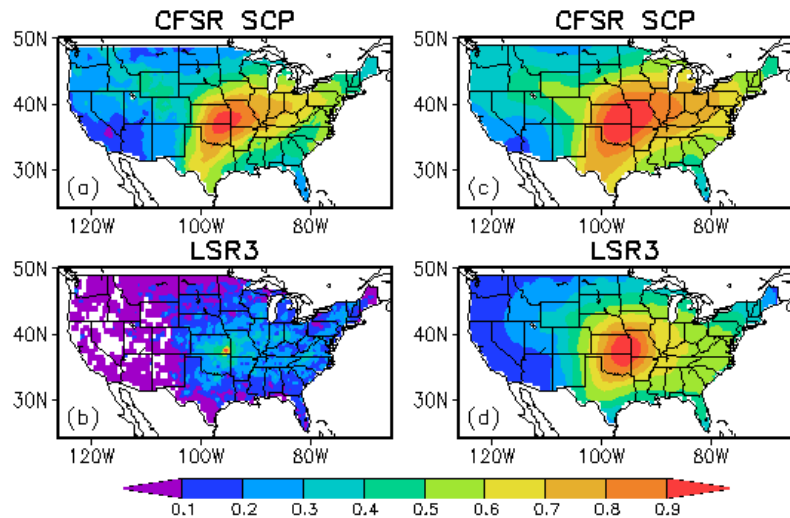


Fig. 4 One-point correlation map between the observed weekly anomaly (1996–2012) at (95.5°W, 37.5°N) and that at each grid point over the U.S. for (a) CFSR SCP and (b) LSR3 at 0.5°x0.5° grid and for (c) CFSR SCP and (d) LSR3 averaged over 5°x5° boxes, respectively.

For comparing the seasonal cycle between observations and GEFS forecast for SCP, Fig. 1 i–l also shows the long-term monthly mean SCP from the GEFS day-1 forecasts. Overall, the model captures the observed seasonality of SCP. For other leads (day-2 to day-14 forecasts), the monthly climatology of SCP slightly decreases with lead time (not shown).

The GEFS forecast skill for SCP is assessed by anomaly correlation (AC) between GEFS SCP and CFSR SCP. The forecast skill decreases with lead time from day 1 to day 14. Particularly, there is a sharp decrease from day 7 to day 8 (not shown). Consistently, the week-2 forecast skill is much lower than week 1, as shown in Fig. 2.

To develop a hybrid forecast model, we first need to establish some relationship between GEFS predicted SCP and observed LSR3. The relationship is the basis for the dynamical-statistical prediction. Given the strong seasonality of both SCP and LSR3 (Fig. 1), a 3-month moving window is used in the analysis. As an example, Fig. 3a–b shows the correlations between observed LSR3 and GEFS week-1 and week-2 forecasts of SCP, respectively, for March, April, and May (MAM), the peak severe weather season. The correlation with the week-2 forecast is less than the week-1 forecast, indicating a weak relationship between GEFS SCP and LSR3 for week 2.

A linear regression model is developed to forecast the number of severe weather (LSR3) using the GEFS predicted SCP as a predictor and based on their relationship depicted in Fig. 3a–b. The forecast skill is cross-validated over the GEFS hindcast period (1996–2012). The anomaly correlation skills (Fig. 3c–d) for week 1 and week 2 are very similar to the corresponding correlations between GEFS SCP and LSR3 (Fig. 3a–b). The forecast skill is low, especially for week 2.

The difficulty in forecasting severe weather is mainly due to its short lifetime and small spatial scale. Figure 4a–b shows the one-point correlation map for weekly CFSR SCP and LSR3, respectively, at the $0.5^\circ \times 0.5^\circ$ grid. It is the correlation map between weekly anomaly at one grid point (here 95.5°W , 37.5°N) and that at every grid point over the U.S. For SCP (Fig. 4a), there are high correlations between the selected grid point and the surrounding grid points, indicating that SCP has a large-scale feature. For LSR3 (Fig. 4b), in contrast, the correlations are small, except the correlation with itself, consistent with the small spatial scale of severe weather. However, when averaging LSR3 over a $5^\circ \times 5^\circ$ box and then recalculating the one-point correlation map, the result (Fig. 4d) shows much higher spatial coherence for LSR3 and is comparable to that of SCP (Fig. 4c).

Next, we use the $5^\circ \times 5^\circ$ area-averaged anomalies to reestablish the relationship between model SCP and observed LSR3. Their

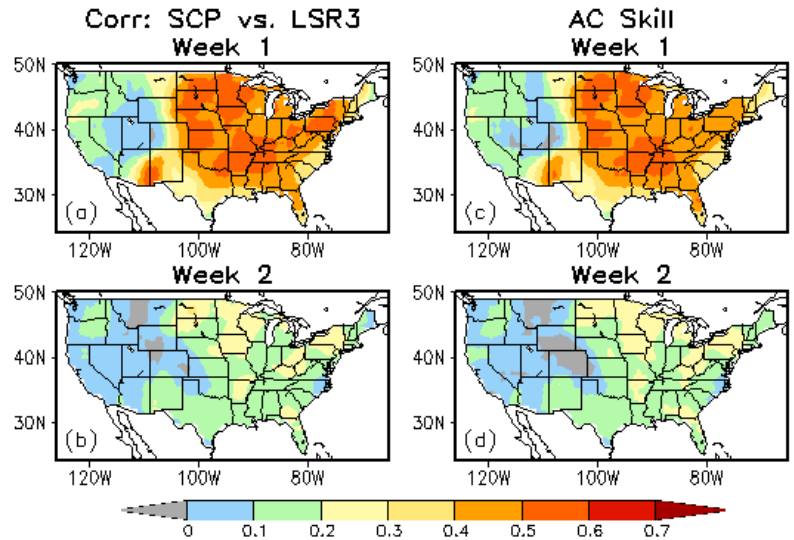


Fig. 5 Same as Fig. 3, but for anomalies averaged over the $5^\circ \times 5^\circ$ box.

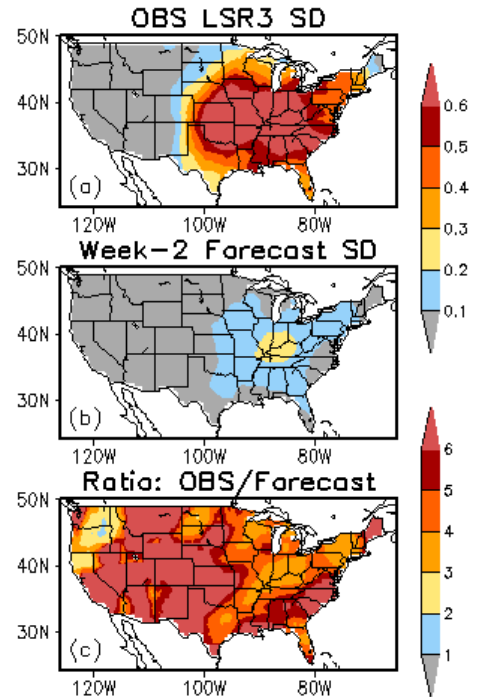


Fig. 6 Standard deviation of (a) observed weekly LSR3 and (b) week-2 forecast and (c) ratio of the observed standard deviation to the week-2 forecast.

correlations (Fig. 5a–b) are much higher than the $0.5^\circ \times 0.5^\circ$ grid (Fig. 3a–b) for both week 1 and week 2. Similarly, the forecast skill of the hybrid model is significantly improved (Fig. 5c–d) by using the $5^\circ \times 5^\circ$ area-averaged anomalies.

Figure 6 shows the spatial distribution of the standard deviation of the observed weekly LSR3 (top) and that of the week-2 forecast (middle) from the hybrid model, respectively, as well as the ratio of the observed standard deviation to the forecast (bottom). The amplitude of the forecasted anomalies is much smaller than the observed. Their ratio is greater than 3 over most of the U.S.

The forecast of the total weekly LSR3 is the hybrid model predicted anomaly plus the observed weekly climatology. Because the amplitude of the forecasted anomalies is much smaller than the observed, the forecast of the total LSR3 tends toward the observed climatology. To avoid this, we can make adjustment for the forecasted anomaly by multiplying it with the ratio in Fig. 6c. In this way, the amplitude of the forecasted anomalies will be closer to the observations. However, this procedure cannot improve the anomaly correlation skill, but may reduce the root-mean-square error of the forecast.

Figure 7 shows an example for the week of May 24 to 30, 2011. On May 24, 2011, there was a tornado outbreak in central and northern Oklahoma. By the end of that day, there were one EF5 tornado, two EF4 and two EF3 tornadoes. Figure 7a is the distribution of weekly total LSR3 with $5^\circ \times 5^\circ$ area-averages. The week-2 forecast and the adjusted forecast are presented in Fig. 7b and 7c, respectively. For this extreme event, some signals in the week-2 forecast are consistent with the observations.

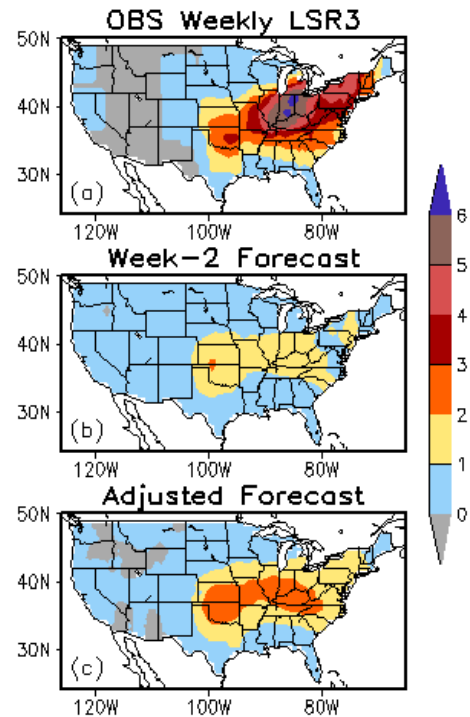


Fig. 7 (a) Observed weekly LSR3, (b) week-2 forecast, and (c) adjusted week-2 forecast for the week of May 24–30, 2011.

4. Conclusions

Following Carbin's work, the Supercell Composite Parameter (SCP) was selected as a variable to represent the large-scale environment and link the model forecast to actual severe weather. The hybrid model forecasts suggest a low skill for week-2 severe weather. However, the forecast can be improved by using the $5^\circ \times 5^\circ$ area-averaged anomalies and the adjustment of the amplitude of the forecasted anomalies.

For future work, we plan to extend the analysis for weeks 3 and 4 using the CFSv2 45-day hindcasts and forecasts. Because the forecast skill for week-2 SCP is already low, we will also need to explore other potential predictors for weeks 3 and 4.

Acknowledgements. We would like to thank our colleagues Brad Pugh, Daniel Harnos, Jon Gottshalck, and Stephen Baxter at CPC for helpful discussions and Yuejian Zhu and Hong Guan at EMC for providing GEFS model forecast data.

References

- Carbin, G. W., M. K. Tippett, S. P. Lillo, and H. E. Brooks, 2016: Visualizing long-range severe thunderstorm environment guidance from CFSv2. *Bull. Amer. Meteor. Soc.*, **97**, 1021–1032.
- Wang H., J.-K. E. Schemm, A. Kumar, W. Wang, L. Long, M. Chellian, G. D. Bell, and P. Peng, 2009: A statistical forecast model for Atlantic seasonal hurricane activity based on the NCEP dynamical seasonal forecast. *J. Climate*, **22**, 4481–4500.